Molecular Dynamics of Monolayer Deposition Using a Nanometer Tip Source

Dong Min Heo,[†] Mino Yang,*[,†] Sungu Hwang,[‡] and Joonkyung Jang*[,§]

Department of Chemistry, Chungbuk National University, Cheongju 361-763, Republic of Korea, Department of Nanomedical Engineering, Pusan National University, Miryang 627-706, Republic of Korea, Department of Nanomaterials Engineering, Pusan National University, Miryang 627-706, Republic of Korea

Received: February 4, 2008; Revised Manuscript Received: March 31, 2008

We performed a molecular dynamics simulation of the monolayer deposition from a nanoscale tip. We investigated how the nascent multilayer droplet around the tip spreads out to become a monolayer on the substrate eventually. A molecule on top pushes out a molecule below it, and the molecule just pushed out in turn pushes out a molecule next to it. The monolayer size grows when such a serial pushing propagates to its periphery. The monolayer periphery shows an initial diffusional growth in its time dependence followed by a slow subdiffusional expansion. We have examined the effects of molecule-substrate binding energy on the shape of the monolayer. For a relatively weak molecule−substrate binding, the monolayer is sparse and has irregular branches. As the molecule−substrate binding strengthens, the monolayer becomes compact and reflects the anisotropy of substrate. A substrate with a hexagonal symmetry results in a hexagonal and a starlike monolayer. An extremely strong molecule−substrate binding removes such an effect of the substrate anisotropy, giving rise to a circular monolayer. The monolayer growth rate exhibits a turn-over behavior with respect to the increase in the molecule−substrate binding strength.

I. Introduction

There has been growing interest in using a nanoscale tip (e.g., an atomic force microscope tip) as a deposition tool of a monolayer thin film on various substrates.[1–9] Because of its sharp asperity, the nanoscale tip serves as a point source of molecules which are designed to bind to a substrate.[7] Despite its widespread use in nanotechnology, little is known about the molecular mechanism and time scale of the monolayer growth using a nanometer tip. The consensus view is that a multilayer droplet should form around the tip due to the continuous downward flux of molecules from the tip (Figure 1). This multilayered nanodroplet subsequently spreads out to form a monolayer. As molecules in the upper layers step down to the substrate, the monolayer periphery broadens on the substrate. Then the question that arises is exactly how this growth occurs? Enunciating this fundamental aspect will serve as a cornerstone for our understanding of the monolayer growth utilizing a nanoscale tip. This fundamental insight will have profound implications for experiments and will be helpful in constructing a realistic model of the monolayer growth.

Suppose molecules are irreversibly trapped by the substrate (e.g., in the case of an extremely strong molecule−substrate binding). Then, for a molecule in the upper layer, the only movement that will lead to a contact with the bare substrate is stepping over the molecules already trapped on the substrate. Once the molecule reaches the periphery of monolayer by moving on top (Figure 1a), it can hop down to one of the binding sites of the substrate and get trapped. As a result, the monolayer grows in size. In the course of hopping down, the molecule might need to overcome an activation energy due to a low coordination number at the monolayer edge (known as the Ehrlich−Schwoebel barrier in epitaxy[10–12]). Our diffusion model for the dip-pen nanolithography (DPN) has been based on this irreversible trapping with hopping mechanism.[7] On the contrary, the previous molecular dynamics (MD) simulation showed that the above hopping mechanism is not the main mechanism for the case relevant to an alkanethiol monolayer on Au (111), a prototypical system of DPN.[13] Instead, a molecule in the upper layer pushes a molecule below out of its place, and the molecule just pushed out in turn pushes a molecule next to it, and so on (Figure 1b). This has been ascribed to the fact that alkanethiols, although tightly bind to gold substrate, can move easily between adjacent 3-fold hollow sites of Au (111).[14] That is, the activation energy for the movement between adjacent hollow sites is small. The previous MD simulation was performed for a small-sized monolayer with a diameter of about 9 nm. Hence, it is not clear whether the above serial pushing mechanism should hold for a big monolayer relevant to experiment. One can imagine that the pushing needs to propagate farther to form a larger monolayer. Then the above serial pushing would require a participation of many molecules, and such a many-body movement might not be feasible. Instead, molecules might opt to move on top of the monolayer as in the hopping down mechanism, Figure 1a.

Herein, we investigate the growth dynamics of monolayer with a size comparable to typical soft nanolithography experiments. For monolayer diameters up to 40 nm, we run MD simulations with trajectory lengths up to 3 ns. We quantitatively study the growth rate of the monolayer periphery. In a recent DPN experiment,[15] it was found that the monolayer shape varies from circular to fractal-like depending on the material and substrate. In principle, the shape of the monolayer island (or domain) would depend on the intermolecular and molecule−substrate interaction energies. In this context, we study how the monolayer shape depends on the molecule−substrate binding energy by systematically varying this energy (but by fixing the intermolecular interaction). Novel features of the monolayer

* To whom correspondence should be addressed. E-mail: MinoYang@chungbuk.ac.kr (M.Y.); jkjang@pusan.ac.kr (J.J.).
[†] Chungbuk National University.
[‡] Department of Nanomedical Engineering, Pusan National University.
[§] Department of Nanomaterials Engineering, Pusan National University.

10.1021/jp801054a CCC: $40.75
Published on Web 05/22/2008

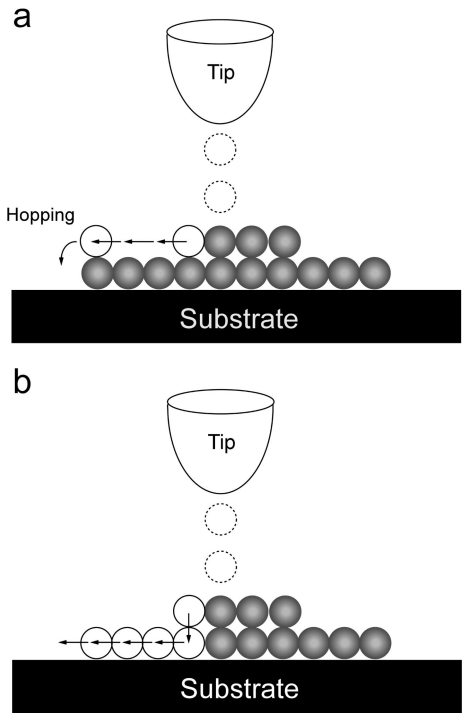

Figure 1. Schematic drawing of the two mechanisms suggested for the monolayer growth. First note that a multilayer droplet forms due to the constant flux of molecules from a nanometer tip (drawn as dotted circles). (a) Hopping down mechanism. For an infinitely strong molecule−substrate binding, molecules get trapped and immobile once they reach one of binding sites on the substrate. The molecule drawn as an open circle in the upper layer can move by stepping over (in the direction of the left arrows) the molecules below (drawn as shaded circles). If the molecule reaches the periphery of the monolayer, it has a chance to hop down to the bare substrate and get trapped. (b) Serial pushing mechanism. The molecule in the upper layer (open circle) pushes the molecule below on the substrate, and the molecule just pushed out in turn pushes a molecule next to it, and so on. The monolayer grows in size when such pushing propagates to the periphery of the monolayer. The arrows represent the moving directions of molecules pushed. In this case, four molecules on the substrate (drawn as open circles) have to move because of the serial pushing initiated by the molecule on top (open circle). The final result of monolayer growth is the same as in part a.

growth emerged from the present large-scale simulation. We show that the substrate anisotropy significantly affects the growth and shape of the monolayer. The growth in the monolayer periphery is found to be composed of two distinct kinetic phases, an initial diffusional and then a slow subdiffusional growth phase, which we name launching and expansion phases, respectively.

II. Simulation Method

As in the prior work,[13] we consider the deposition of nonpolar and spherical molecules on Au(111) substrate. The molecular mass is set identical to that of 1-octadecanethiol ($CH_3(CH_2)_{17}SH$, ODT), which is the prototypical molecule in DPN.[1,2,15] By consideration of its spherical shape, our molecular model is only remotely related to ODT. In ref 13, however, we have found that this coarse-grained model captures the essential features of a realistic MD simulation. That is, we have performed a simulation that explicitly takes into account the alkyl chain of ODT (by using a united atom model) as well as the sulfur−Au bond (by using a Morse potential[14,16,17] fitted to experiments[18]). Such a realistic simulation was in qualitative agreement with our coarse grained simulation. In a similar vein, Mahaffy et al.[16] showed that coarse-graining butanethiolate as a spherical molecule yields a nearly identical value in its surface diffusion constant on the Au(111) surface.

Our nanoscale tip is modeled as a cylinder made of silicon atoms. ODT molecules reside inside the cylinder, mimicking the so-called "fountain-pen tip" used in DPN.[19] We have studied a spherical tip coated with ODT molecules and obtained similar results. Therefore, we only report the case of the cylindrical tip here. Every interaction (molecule−molecule, molecule−tip atom, and molecule−Au atom interactions) is assumed to be of a pairwise Lennard-Jones (LJ) potential,[20] $U(r) = 4\varepsilon[(\sigma/r)^{12} - (\sigma/r)^6]$.We take LJ parameters, ε and σ, for the tip atom (silicon) and molecule as 0.4184 kJ/mol and 0.4 nm[21] and 5.24 kJ/mol and 0.497 nm, respectively. The LJ parameter ε of our molecule is taken from that of stearic acid ethyl ether,[22] which is similar to ODT in mass. We chose the LJ size parameter σ (0.497 nm) of our molecule to reproduce the well-known structure of the ODT monolayer on Au (111).[23] We take σ for gold as 0.2655 nm reported in the literature,[24] but the ε value for gold is systematically varied in order to examine the effects of molecule-substrate binding energy. The Lorentz−Berthelot combination rule[20] is used for the interactions between unlike atomic or molecular species. The strength of molecule−substrate binding can be quantified by the LJ parameter, ε_b, for molecule-gold interaction potential. Zhang et al.[17] modeled the ODT−gold interaction as a Morse potential and fitted the potential parameters to experimental binding energies. The dissociation energy of the Morse potential ε_0 was found to be 3.182 kcal/mol. We have set the lowest value of our LJ energy parameter ε_b identical to ε_0. To inspect the effects of the molecule−substrate binding strength, we have considered seven additional values of ε_b, which are taken to be multiples of ε_0 ($2\varepsilon_0$, $3\varepsilon_0$, $4\varepsilon_0$, $5\varepsilon_0$, $6\varepsilon_0$, $7\varepsilon_0$, and $8\varepsilon_0$). One can certainly think of the ε_b value smaller than ε_0, but such ε_b would be less relevant to a typical soft nanolithography which adopts molecules strongly bind to the substrate so that the resulting monolayer is stable.

The radius and height of our cylindrical tip are 8.0 and 24.1 nm, respectively. Before starting the simulation of molecular deposition, we put 5754 molecules inside the cylinder by sealing its bottom and top. We equilibrated the molecules inside the tip by running an MD simulation for 500 ps at room temperature. We then cut the bottom part of the cylinder so that 250−300 molecules protrude from the open end of the cylinder (Figure 2). In doing so, we also removed some molecules close to the substrate so that the total number of molecules inside the tip is now 5602. The vertical distance from the tip end to the substrate is 1.3 nm. We include only a single layer of Au(111) substrate in simulation, which might underestimate the molecular attraction of the substrate. By consideration of the qualitative nature of the present work, however, we content ourselves with this single-layer description of the substrate. The horizontal boundary of the gold substrate is a circle with a lateral diameter of 63.9 nm, and the substrate consists of 44815 gold atoms. The tip and gold atoms are frozen during simulation but they interact with molecules through LJ potentials. We propagated the molecular trajectory by using the velocity Verlet algorithm.[20] We used a time step of 1 fs, and the total time length of simulation was 3 ns. The temperature of our system was fixed to 300 K by using the thermostat proposed by Berendsen et al.[25]

III. Results and Discussion

We first describe our observation of the molecular mechanism of the monolayer growth. By carefully examining the side-view

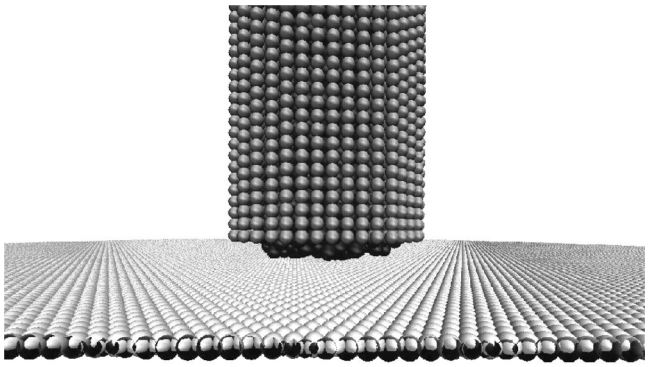

Figure 2. The initial configuration of molecular dynamics simulation. Total of 5602 molecules initially reside in a cylindrical tip (made of silicon atoms) above the Au(111) surface (a single layer consisting of 44815 atoms). The vertical distance from the tip end to the surface is 1.3 nm. The radius and height of our cylinder tip are 8.0 and 24.1 nm, respectively. The gold surface has a circular boundary with a diameter of 63.9 nm. One can see the protrusion of molecules at the end of the open cylindrical tip.

molecular dynamics snapshots taken in the course of the monolayer growth, we conclude that virtually no molecule reaches the periphery by moving on top of the molecules already adsorbed on the substrate as in the hopping down model, Figure 1a. The Supporting Information provides an animation that illustrates the observed growth mechanism. We found one exception in the case of $\varepsilon_b = 5\varepsilon_0$, however. There, we observed that one molecule slides very fast on top of the monolayer straight to the periphery. It then hops down to the substrate to sit on one of the 3-fold hollow sites (center of three gold atoms) of the substrate. Except for this one occasion, molecules typically stayed on top of other molecules for several picoseconds (3−4 ps) and then pushed molecules below them to make their ways down to the substrate. The pushing mechanism holds even for a monolayer as large as 40 nm in diameter and for the strongest molecule−substrate binding energy considered in this work, $\varepsilon_b = 8\varepsilon_0$. For binding energies of $7\varepsilon_0$ and $8\varepsilon_0$, more molecules are found to move on top of the monolayer. They execute the on-top movement up to nearly halfway to the periphery and then the pushed molecules below on the substrate, touching the bare substrate. Therefore, the growth in this case occurs through a combination of the moving on top in Figure 1a and the serial pushing in Figure 1b.

In Figure 3, we present four representative MD snapshots of the growing monolayer (top view) for the lowest molecule−substrate binding energy, $\varepsilon_b = 3.182$ kcal/mol. Snapshots are taken at 200 ps (a), 1 ns (b), 2 ns (c), and 3 ns (d). The tip is not drawn for visual clarity. For this relatively weak molecule−substrate binding, molecules easily move between the binding sites of the substrate. In addition to the main island at the center, one can see that many molecules are scattered individually or in the form of small islands. These small islands are unstable and are constantly fluctuating in shape.

We have examined the case of a molecule-substrate binding energy four times bigger than in Figure 3 ($\varepsilon_b = 12.73$ kcal/mol). Figure 4 shows that the growth kinetics in such a case is quite different from that in Figure 3. Overall, scattered small islands of molecules or isolated molecules are dramatically reduced in number. The monolayer grows as a compact island all the time. Occasionally, small holes appear in the monolayer, but they are quickly (within several picoseconds) filled up by the molecules nearby or by the incoming molecules from the tip. Since the molecules are strongly attracted to the substrate, one might expect that individual molecules on the substrate are

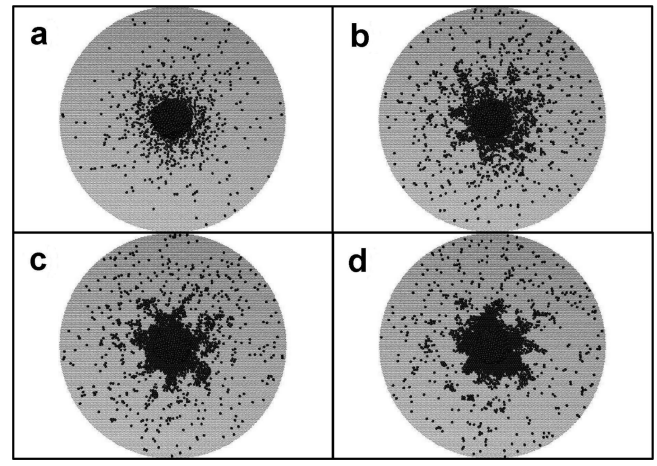

Figure 3. Representative snapshots of the monolayer growth on the substrate. In this and all the following figures, only molecules and the substrate atoms are drawn for visual clarity (top view). The molecule−surface binding energy ε_b is 3.182 kcal/mol, the smallest value considered in the present work. Snapshots are taken, respectively, at $t = 200$ ps (a), 1 ns (b), 2 ns (c), and 3 ns (d).

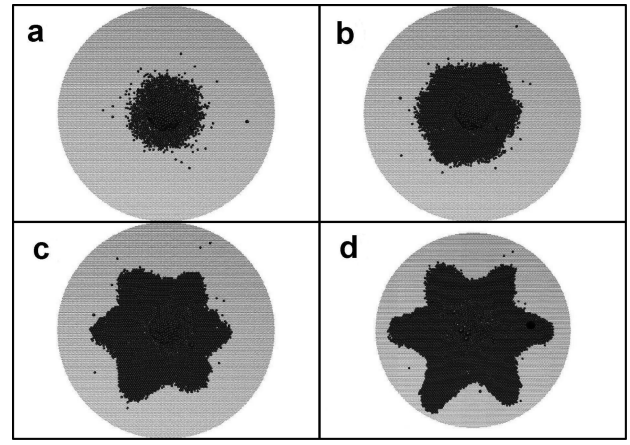

Figure 4. Representative snapshots of the monolayer growth on the substrate (top view) for a molecule−substrate binding energy 4 times bigger than in Figure 3 ($\varepsilon_b = 12.73$ kcal/mol). Snapshots are taken, respectively, at $t = 200$ ps (a), 1 ns (b), 2 ns (c), and 3 ns (d).

less mobile and the growth rate of the monolayer should be slower than in the case of Figure 3. However, as we discussed above, the growth rate of the monolayer is not just determined by the speed of individual molecule on the substrate but also by the attractive force pulling down the molecules from the tip. An increased molecular attraction from the substrate can lead to a faster flow of molecules from the tip to the substrate, which in turn can increase the growth rate of the monolayer. Also, an increased molecule−substrate binding makes the growing monolayer compact as opposed to the case where the monolayer is constantly broken into small islands (as for a weak molecule−substrate binding, Figure 3). The monolayer growth in Figure 4 turns out to be faster than that of Figure 3. If one compares the monolayer sizes of Figures 3 and 4 for a given time, one can see that the monolayer size in figure 4 is always bigger than in Figure 3.

Note that the monolayer in Figure 4 is circular initially (Figure 4a) but becomes noncircular at later times (parts b−d of Figure 4). Initially, molecules easily move from one of the hollow binding sites (the centers of 3 gold atoms) to another regardless of their moving direction on the substrate. As the monolayer gets bigger at later times however, the monolayer growth requires a longer series of pushing according to the pushing

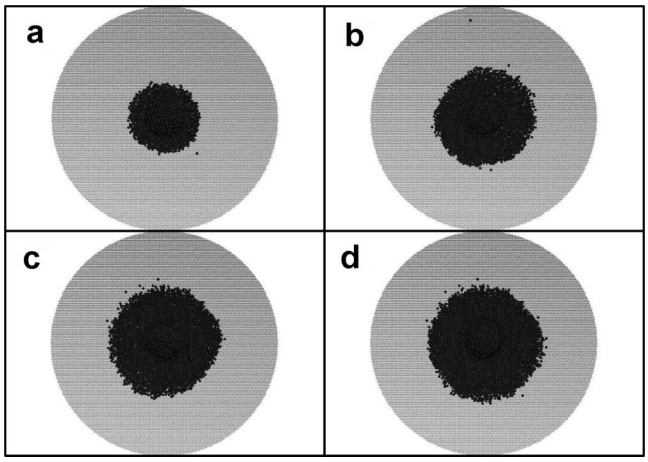

Figure 5. Representative snapshots of the monolayer growth on the substrate (top view) for a molecule−substrate binding energy 8 times bigger than in Figure 3, (ε_b = 25.46 kcal/mol). Snapshots are taken, respectively, at t = 200 ps (a), 1 ns (b), 2 ns (c), and 3 ns (d).

mechanism, Figure 1b. A long serial pushing calls for a cooperation of many molecules on the substrate. Now the moving direction becomes important in the monolayer growth, and the substrate anisotropy (6-fold rotational symmetry) plays a significant role in determining the monolayer growth directions. As shown in Figure 4b, by the time of 1 ns, the monolayer periphery becomes hexagonal in shape. This implies that the monolayer grows faster in the direction from the center to one of six vertices of the hexagon. Along these six directions, a molecule sitting at one of the binding sites can move to an adjacent binding site with relative ease. If we imagine a straight molecular path in going from one binding site to adjacent one, a molecule can pass through the valley between two gold atoms after it climbs over a gold atom. In other directions however, a molecule has to move (nearly) on top of gold atoms all the time during its transit from one binding site to another. We think the passing through the valley facilitates the growth along the six directions toward the vertices. At early times, when the number of molecules involved in the serial pushing is small, the energy barrier required for the lateral movement on the substrate is small and is not substantially dependent on direction. Therefore the monolayer growth is isotropic. As the number of molecules involved in the monolayer growth increases at later times, the energy barrier of the molecular movement from one binding site to another becomes large and depends significantly on direction. Now molecules strongly prefer the above six directions in moving, giving a hexagonal monolayer shape (Figure 4b). A further increase in time makes the growth along these preferred directions even faster. By the time of 2 ns (Figure 4c), the periphery becomes a starlike pattern. As time increases from 2 to 3 ns, the starlike feature becomes more eminent (Figure 4d).

Figure 5 shows the case of the strongest molecule-substrate binding considered, ε_b = 25.46 kcal/mol. Here, the monolayer periphery assumes a compact circular shape at all times. Notice a hexagonal or starlike pattern due to the substrate anisotropy in Figure 4 does not exist. Because of an extremely strong molecule−substrate binding, the molecular motion on the substrate is sluggish. The movement from one binding site to another takes more energy than in the previous cases. The difference in the activation energy depending on direction however becomes relatively small compared to the activation energy itself. As a result, the molecular motion becomes isotropic and the monolayer periphery becomes circular. One

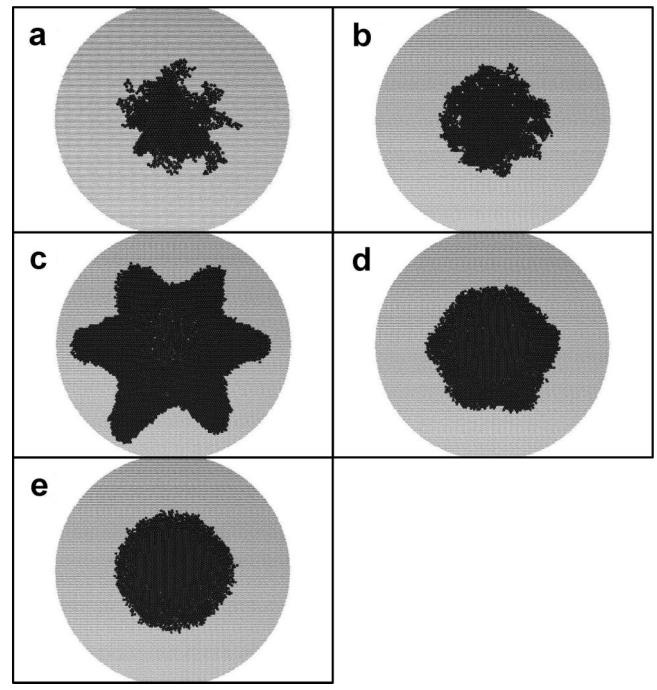

Figure 6. Final monolayer shapes for various molecule−substrate binding energies, ε_bs. We have drawn snapshots taken at t = 3 ns for five different binding energies, $\varepsilon_b = \varepsilon_0$ (a), $2\varepsilon_0$ (b), $4\varepsilon_0$ (c), $6\varepsilon_0$ (d), and $8\varepsilon_0$ (e).

can also think of this in terms of the surface energy of the monolayer. In the case of the largest molecule−substrate binding energy, the surface energy of the monolayer becomes a dominating factor in determining its shape, resulting in a circular monolayer which minimizes its surface-to-volume ratio (in this case, the ratio of the periphery length to the monolayer area). The molecular mobility on the substrate in this case is low so that a molecule on top cannot easily push out a molecule below on the substrate. The molecules dropped from the tip move on the monolayer for a while (4−5 ps). A significant number (about 100) of molecules stay on top of the monolayer even after 3 ns. No molecule on top however is found to reach the periphery of the monolayer and hop down to the bare substrate. Instead, a molecule on top typically steps over several molecules and then pushes out one of molecules on the substrate to make its way to the substrate. As discussed above, a typical molecule in this case performs a combination of the on-top motion in Figure 1a and the subsequent pushing in Figure 1b.

We explained the hexagonal (Figure 4) and circular (Figure 5) monolayer shapes in terms of the directional difference of the energy barrier for the molecular motion from one binding site to another. We need to point out this explanation is a postulate, although plausible, that needs a proof. A rigorous, quantitative proof of our postulate would require the actual calculation of the energy barrier depending on direction. Here, the molecular motion is not a movement of a single molecule on the substrate. In principle, it involves a movement of all the molecules on the substrate. Evaluating the corresponding energy barrier requires constructing a multidimensional energy surface that takes into account the coordinates of all the molecules. Such an intensive computation is beyond the scope of this work. It would be an interesting ramification of the present work.

Figure 6 summarizes how the molecule−substrate binding strength affects the shape of nanosized monolayer. The final structure of monolayer is drawn for various molecule−substrate binding energies, ε_bs. When the binding energy is small (ε_b =

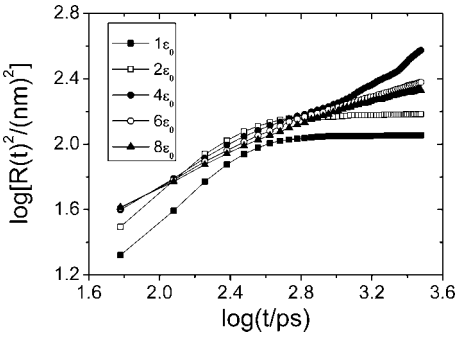

Figure 7. Log−log plot of the radius squared of the monolayer $R(t)^2$ as a function of time t. $\log[R(t)^2]$ vs $\log(t)$ are drawn for the molecule−substrate binding energies of ε_0 (filled squares), $2\varepsilon_0$ (open squares), $4\varepsilon_0$ (filled circles), $6\varepsilon_0$ (open circles), and $8\varepsilon_0$ (filled triangles). Lines are drawn for guidance of eyes.

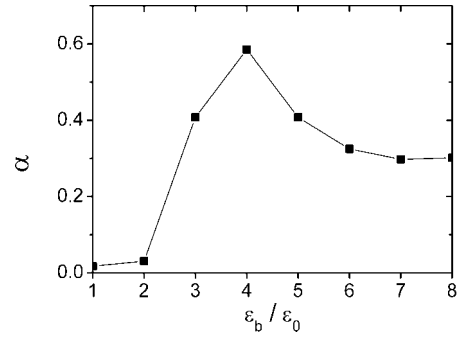

Figure 8. The time exponent of $R(t)^2$ in the expansion phase α as a function of the molecule−substrate binding energy, ε_b. For each binding energy, $R(t)^2$ in the expansion phase (Figure 7) has been fitted by the function t^α and the exponent α has been determined by the least-squares method. The exponent α is plotted as a function of the binding energy. Lines are drawn to guide eyes.

3.182 kcal/mol, Figure 6a), the monolayer pattern is quite irregular and has many branches. This is in qualitative agreement with the recent DPN experiment using 1-dodecylamine on mica.[15] As the binding strength increases (ε_b = 6.364 kcal/mol, Figure 6b), the irregular branches of the monolayer disappear and molecules aggregate to form a compact pattern. The monolayer however is not perfectly compact but has some holes. Further increasing the molecule-substrate binding strength (ε_b = 12.73 kcal/mol, Figure 6c) leads to an interesting starlike shape. As discussed above, this anisotropic pattern arises from the fact that the molecular motion from the center to one of hexagon vertices requires small activation energy due to the surface anisotropy of Au(111). If we further increase the binding energy (ε_b = 19.10 kcal/mol, Figure 6d), the final structure becomes a hexagon. Hence, we see that the fast monolayer growth from the center to vertex is less pronounced than in Figure 6c. An increased molecule−substrate binding strength in this case gives rise to an increased activation energy for the molecular movement from one binding site to another. On the other hand, the difference in the activation energy depending on direction becomes relatively small compared to the activation energy itself. Then the preference of the center-to-vertex movement diminishes, but it still plays a role to give a hexagonal monolayer. In the case of the largest binding energy (ε_b = 25.46 kcal/mol, Figure 6e), the monolayer structure is circular. The activation energy for molecular movement from one binding site to another is even higher than in Figure 6d. The difference in the activation energy depending on direction becomes negligible compared to the activation energy itself. Therefore, the molecular movement is equally likely for all directions, leading to an isotropic growth shown in Figure 6e.

We now quantitatively study the growth rate of the monolayer radius. During simulation, we kept track of the number of molecules that constitute the biggest main island at a given time t, $N(t)$. Counting $N(t)$ is not trivial. We first chose molecules whose vertical distances from the substrate are within 0.45 nm. Among such molecules, we checked the intermolecular distance of every possible pair and declared the pairs with intermolecular distances below 0.95 nm as neighbors. A molecule is treated as a part of the island if it is a neighbor of *any* molecule that forms the island. Then the monolayer radius at time t, $R(t)$, is defined as $R(t)^2 = N(t)/(\pi\rho)$, where ρ is the surface density of the perfectly aligned monolayer (4.64 nm^{-2}). In Figure 7, we draw the radial growth of the monolayer for five values of the binding strengths, ε_bs. The figure shows the log−log plot of $R(t)^2$ vs t. There are two distinct phases in the growth of the monolayer radius. We name these as the launching and expansion phases, respectively. During the initial launching phase, molecules flow down fast from the tip and move rapidly on the substrate. The rareness of other molecules on the substrate allows molecules landed on the substrate to move without noticeable resistance. This launching phase persists until the area directly under the tip is completely covered with molecules. Then the growth in the monolayer periphery enters an expansion phase where the nascent monolayer around the tip expands slowly. For the expansion of the monolayer, it takes a series of pushing that needs to propagate to the periphery. Sometimes, it is found that many molecules move collectively toward the periphery to expand the monolayer. The molecular motion and the monolayer growth in the expansion phase are significantly slower than in the initial launching phase. One can see that, for all the binding strengths, the slope of $\log[R(t)^2]$ decreases at around $\log(t) = 2.7$. That is, after about 500 ps, the radial growth slows down, signaling that the monolayer growth has entered the expansion phase. In the launching phase, the power law exponent α for the time dependence of $R(t)^2(\propto t^\alpha)$ is close to 1, especially for the two smallest binding energies, $\varepsilon_b = \varepsilon_0$ and $2\varepsilon_0$. The monolayer periphery growth is diffusional in the sense that its radius squared $R(t)^2$ shows a linear dependence on time. Interestingly, the diffusion theory assuming the hopping down mechanism in Figure 1a also predicts a diffusional time dependence.[7] In the expansion phase, the power law exponent α for the time dependence of $R(t)^2(\propto t^\alpha)$ is smaller than one (ranging from about 0.2 to 0.7). This growth rate can be called subdiffusional in its time dependence. Nanoscopically, the pushing of molecule in the expansion phase needs to propagate over a longer distance in order to enlarge the monolayer periphery. Such a long series of pushing naturally takes more time than the pushing in the launching phase.

Figure 8 shows how the growth rate of the monolayer radius depends on the binding energy ε_b. In creating the figure, we leave out the initial launching phase and only focus on the expansion phase. Drawn in the figure is the exponent of the radius growth α above as a function of the binding energy ε_b. We used the least-squares fitting to obtain the growth exponent numerically. The figure clearly shows a turn-over behavior of the growth rate with respect to ε_b. Up to the binding energy of $4\varepsilon_0$, increasing the binding strength raises the monolayer growth rate. This means that an enhanced attractive force of the substrate pulls down molecules from the tip more strongly, making the downward molecular flow from the tip faster. A further increase in the binding strength however makes the growth rate smaller. Because of a very strong molecule−substrate binding strength, molecules are now less mobile than for a smaller binding energy. The pushing of a molecule from the center toward the periphery takes more energy due to the strong molecular binding to the

substrate. The molecule−substrate binding energy of $4\varepsilon_0$ turns out to give the fastest growth in the monolayer radius.

IV. Conclusions

Soft nanolithography using a nanoscale scanning probe tip (e.g., DPN) is widely used in nanotechnology. By consideration of its wide applications, we need to understand clearly the molecular mechanism of this technique and the time scale of the monolayer growth. In this context, we have performed molecular dynamics simulations to study the growth mechanism and the time rate and the shape of the monolayer deposited from a nanoscale tip. By use of the coarse-grained molecular model that captures the essential features of alkanethiol, we have examined the monolayer growth dynamics. The serial pushing mechanism found in our previous study of a small-sized monolayer holds for a monolayer with a diameter up to 40 nm. That is, molecules deposited from the tip push out molecules below already on the substrate, and molecules pushed out in turn push other molecules nearby. When such a pushing propagates to the periphery, sometimes in a collective manner, the monolayer grows in size. We have investigated how the monolayer periphery shape is affected by the molecule−substrate binding energy. For a weak binding energy, the monolayer is limited in size and has irregular branches. As the binding strength increases, the monolayer becomes compact and dense, consistent with experimental observations in DPN.[15]

The present long-time (3 ns), large-scale (40 nm diameter) simulation revealed novel features which could not be seen in the previous small-sized (8-nm diameter), short-time (600 ps long) simulation. We found the monolayer becomes hexagonal or starlike due to the substrate anisotropy for a moderate molecule−substrate binding strength. An extremely strong molecule−substrate binding erases this anisotropy effect, giving a circular periphery. Dynamically, the deposition from the tip and the subsequent monolayer growth occur in two phases. During the launching phase at early times, molecules in the tip are pulled down by the attractive force of the substrate and quickly spread out. The monolayer radius shows a diffusional time dependence. This launching phase is followed by the expansion phase. Since the area around the tip is already covered by a monolayer, it is more difficult for a molecule dropped from the tip to push out molecules on the substrate. The growth of periphery requires a collective molecular motion or a series of pushing of molecules. This significantly slows down the monolayer growth. Interestingly, the speed of monolayer growth during the expansion phase shows a turnover behavior with respect to the increase in the molecule−substrate binding strength. The growth speed initially increases with raising the molecule−substrate binding strength, reflecting the enhanced attraction from the substrate. A further rise in the binding strength however slows down the growth. This means that an extremely strong binding strength can make molecules immobile and block the propagation of molecular pushing toward the periphery.

The conclusions of the present work have significant implications for soft nanolithography utilizing a nanometer tip. For example, we have shown that the monolayer growth speed and its shape can be changed drastically by varying the substrate-molecule binding strength. The molecular mechanism of monolayer growth found in the current work will be useful in a further modeling of soft nanolithography. To emulate real experiments, however, there are many aspects that need to be taken into account. For a moving tip such as a scanning AFM tip, we need to consider the moving speed of the tip. Under humid conditions, there is a strong capillary force due to the presence of a water droplet between the tip and substrate.[26] The meniscus is considered as the channel for the molecular transport from the tip to the substrate. Depending on whether the molecule is hydrophilic or hydrophobic, the tip-to-substrate molecular flow can be facilitated or resisted by the presence of the meniscus. In addition, a humidity variation will change the meniscus size and therefore affect the monolayer growth. For a hydrophilic tip, there will be a strong capillary force that should make the molecular flow faster. It needs a further study to figure out exactly how these factors manifest themselves in the monolayer growth. The present work will serve as a starting point of such an advanced modeling of soft nanolithography.

Supporting Information Available: An animation illustrating the molecular dynamics simulation of the ODT (blue spheres) monolayer growth on Au(111) (drawn as yellow spheres). The cylindrical tip is not drawn for visual clarity. The side view clearly shows that the monolayer grows by the serial pushing mechanism in Figure 1b. The molecule−substrate binding energy ε_b is 15.91 kcal/mol. The time interval between two consecutive snapshots is 1.25 ps. This material is available free of charge via the Internet at http://pubs.acs.org.

Acknowledgment. This work was supported by the Korea Research Foundation Grant funded by the Korean Government (MOEHRD, Grant No. 2005-070-C00065). M.Y. acknowledges financial support from KRF (KRF-2003-070-C00026).

References and Notes

(1) Mirkin, C. A. *ACS Nano* **2007**, *1*, 79.
(2) Huck, W. T. S. *Angew. Chem., Int. Ed.* **2007**, *46*, 2754.
(3) Ginger, D.; Wei, J. H. *Small* **2007**, *3*, 2034.
(4) Nafday, O. A.; Vaughn, M. W.; Weeks, B. L. *J. Chem. Phys.* **2006**, *125*, 144703.
(5) Cho, Y.; Ivanisevic, A. *Langmuir* **2006**, *22*, 8670.
(6) Cho, N.; Ryu, S.; Kim, B.; Schatz, G.; Hong, S. *J. Chem. Phys.* **2006**, *124*, 024714.
(7) Jang, J.; Hong, H.; Schatz, G. C.; Ratner, M. A. *J. Chem. Phys.* **2001**, *115*, 2721.
(8) Jaschke, M.; Butt, H.-J. *Langmuir* **1995**, *11*, 1061.
(9) Noy, A.; Miller, A. E.; Klare, J. E.; Weeks, B. L.; Woods, B. W.; DeYoreo, J. J. *Nano Lett.* **2002**, *2*, 109.
(10) Shin, B.; Aziz, M. J. *Phys. Rev. B* **2007**, *76*, 165408.
(11) Li, S.-C.; Han, Y.; Jia, J.-F.; Xue, Q.-K.; Liu, F. **2006**, 74, 195428.
(12) Johansen, C. G.; Huang, H.; Lu, T.-M. *Appl. Phys. Lett.* **2007**, *91*, 121914.
(13) Ahn, Y.; Hong, S.; Jang, J. *J. Phys. Chem. B* **2006**, *110*, 4270.
(14) Beardmore, K. M.; Kress, J. D.; Gronbech-Jensen, N.; Bishop, A. R. *Chem. Phys. Lett.* **1998**, *286*, 40.
(15) Manandhar, P.; Jang, J.; Schatz, G. C.; Ratner, M. A.; Hong, S. *Phys. Rev. Lett.* **2003**, *90*, 115505.
(16) Mahaffy, R.; Bhatia, R.; Garrison, F. J. *J. Phys. Chem. B* **1997**, *101*, 771.
(17) Zhang, L.; Goddard, W. A., III; Jiang, S. *J. Chem. Phys.* **2002**, *117*, 7342.
(18) Dubois, L. H.; Nuzzo, R. G. *Annu. Rev. Phys. Chem.* **1992**, *43*, 437.
(19) Deladi, S.; Tas, N. R.; Berenschot, J. W.; Krijnen, G. J. M.; de Boer, M. J.; de Boer, J. H.; Peter, M.; Elwenspoek, M. C. *Appl. Phys. Lett.* **2004**, *85*, 5361.
(20) Allen, M. P.; Tildesley, D. J. *Computer Simulation of Liquids*; Clarendon Press; Oxford, 1987.
(21) Zhang, L.; Jinag, S. *J. Chem. Phys.* **2002**, *117*, 1804.
(22) Zhou, J.; Lu, X.; Wang, Y.; Shi, J. *Fluid Phase Equlib.* **2000**, *172*, 279.
(23) Alves, C. A.; Smith, E. L.; Porter, M. D. *J. Am. Chem. Soc.* **1992**, *114*, 1222.
(24) Zhang, L.; Balasundaram, R.; Gehrke, S. H.; Jiang, H. *J. Chem. Phys.* **2001**, *114*, 6869.
(25) Berendsen, H. J. C.; Postma, J. P. M.; van Gunsteren, W. F.; DiNola, A.; Haak, J. R. *J. Chem. Phys.* **1984**, *81*, 3684.
(26) (a) Jang, J.; Sung, J.; Schatz, G. C. *J. Phys. Chem. C* **2007**, *111*, 4648. (b) Jang, J.; Yang, M.; Schatz, G. C. *J. Chem. Phys.* **2007**, *126*, 174705.

JP801054A